Edohedral Fullerenes

Methane as a Selectivity Booster in the Arc-Discharge Synthesis of Endohedral Fullerenes: Selective Synthesis of the Single-Molecule Magnet Dy$_2$TiC@C$_{80}$ and Its Congener Dy$_2$TiC$_2$@C$_{80}$

Katrin Junghans, Christin Schlesier, Aram Kostanyan, Nataliya A. Samoylova, Qingming Deng, Marco Rosenkranz, Sandra Schiemenz, Rasmus Westerström, Thomas Greber, Bernd Büchner, and Alexey A. Popov*

Abstract: The use of methane as a reactive gas dramatically increases the selectivity of the arc-discharge synthesis of M-Ti-carbide clusterfullerenes (M = Y, Nd, Gd, Dy, Er, Lu). Optimization of the process parameters allows the synthesis of Dy$_2$TiC@C$_{80}$-I and its facile isolation in a single chromatographic step. A new type of cluster with an endohedral acetylide unit, M$_2$TiC$_2$@C$_{80}$, is discovered along with the second isomer of M$_2$TiC@C$_{80}$. Dy$_2$TiC@C$_{80}$-(I,II) and Dy$_2$TiC$_2$@C$_{80}$-I are shown to be single-molecule magnets (SMM), but the presence of the second carbon atom in the cluster Dy$_2$TiC$_2$@C$_{80}$ leads to substantially poorer SMM properties.

The field of endohedral metallofullerene (EMF) research was revolutionized in 1999, when it was discovered that the presence of small amounts of nitrogen gas in the arc-discharge generator afforded Sc$_3$N@C$_{80}$, a new type of EMF with a trimetalnitride cluster inside the carbon cage.[1] The use of NH$_3$ as a reactive gas instead of molecular nitrogen resulted in much higher selectivity in the synthesis of nitride clusterfullerenes as the yield of empty fullerenes in such conditions decreased dramatically.[2] Discovery of nitride clusterfullerenes triggered exhaustive studies of other clusterfullerenes, resulting in a variety of EMF families with endohedral S,[3] O,[4] C$_2$,[5] CH,[6] CN,[7] and other nonmetal units.[8]

One of the advantages of the trimetallic cluster in nitride clusterfullerenes is the possibility of combining two or even three different metals within one EMF molecule. Mixed-metal nitride clusterfullerenes may exhibit new properties not present in homometallic nitride clusterfullerenes. Examples include unusual redox behavior,[9] stabilization of unconventional carbon cages,[10] and strong variation of chemical reactivity[11] and magnetization behavior[12] depending on the number of lanthanide ions in the cluster. However, a disadvantage of the mixed-metal EMFs is the increased complexity of their chromatographic separation.

Whereas nitride clusterfullerenes are usually formed with Group III metals, such as Sc, Y, and trivalent lanthanides,[13] Yang et al. demonstrated that a single Ti ion can be introduced into the mixed-metal nitride cluster together with Sc or Y.[14] Due to the trivalent Ti, M$_2$TiN@C$_{80}$ clusterfullerenes have unusual electronic and chemical properties.[15] Recently, in an attempt to obtain Ti-based nitride clusterfullerenes with Lu using NH$_3$ as a reactive gas or melamine as a solid organic nitrogen source, we have discovered a new type of clusterfullerene, Lu$_2$TiC@C$_{80}$, which has an endohedral μ$_3$-carbide ion and a Ti−C double bond.[16] The molecule is an isostructural analogue of Lu$_2$ScN@C$_{80}$, in which the Sc–N fragment is replaced by the isoelectronic Ti=C fragment. Unfortunately, in the Lu/Ti/NH$_3$ and Lu/Ti/melamine syntheses, Lu$_2$TiC@C$_{80}$ is only a minor by-product; the products are predominantly Lu$_3$N@C$_{2n}$ nitride clusterfullerenes, which precludes further exploration of this new type of clusterfullerenes. Herein we demonstrate that 1) M$_2$TiC@C$_{80}$ clusterfullerenes can be synthesized with high selectivity for many lanthanides using methane as a reactive gas; 2) this synthetic route also affords appreciable amounts of another cage isomer of M$_2$TiC@C$_{80}$ as well as a new type of clusterfullerenes, M$_2$TiC$_2$@C$_{80}$; 3) Dy$_2$TiC@C$_{80}$ exhibits single-molecule magnet (SMM) behavior, whereas the SMM properties of Dy$_2$TiC$_2$@C$_{80}$ are are less pronounced owing to the presence of the second carbon atom in the central unit.

EMFs were obtained by arc-discharge synthesis under He atmosphere with a small amount of CH$_4$ gas using graphite rods packed with a mixture of Ti, lanthanide (Y, Ce, Nd, Gd, Dy, Er, or Lu), and a graphite powder. The role of CH$_4$ in this type of synthesis is similar to that of NH$_3$[2] in the synthesis of nitride clusterfullerenes: the reactive gas increases selectivity of the process by suppressing the formation of empty fullerenes and making the EMFs with desired central atom(s) the main products. Figure 1 shows that under optimized conditions, carbide clusterfullerenes are

[*] K. Junghans, C. Schlesier, N. A. Samoylova, Q. Deng, M. Rosenkranz, S. Schiemenz, Prof. Dr. B. Büchner, Dr. A. A. Popov
Leibniz Institute for Solid State and Materials Research
Helmholtzstrasse 20, 01069 Dresden (Germany)
E-mail: a.popov@ifw-dresden.de

A. Kostanyan, Dr. R. Westerström, Prof. Dr. T. Greber
Physik-Institut der Universität Zürich
8057 Zürich (Switzerland)

A. Kostanyan
Swiss Light Source, Paul Scherrer Institut
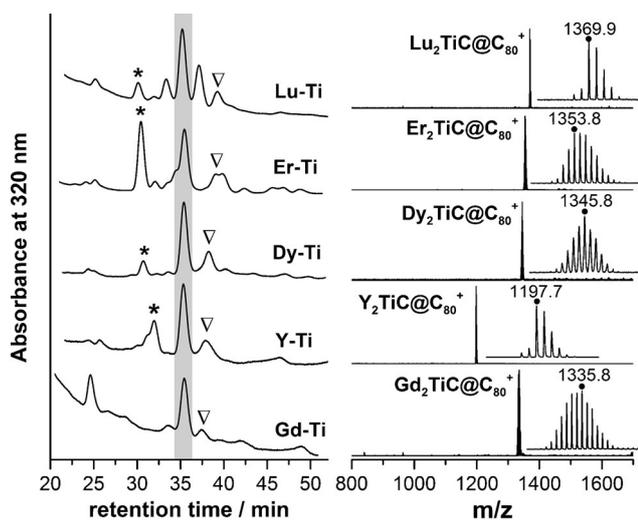5232 Villigen PSI (Switzerland)

Figure 1. Left: HPLC chromatograms of raw extracts obtained in metal/Ti/CH$_4$ arc-discharge syntheses (Buckyprep column, toluene as eluent); asterisks mark the fractions with M$_3$N@C$_{80}$, shaded rectangle highlights the fractions with M$_2$TiC@C$_{80}$-I, whereas triangles denote the fractions with M$_2$TiC@C$_{80}$-II/M$_2$TiC$_2$@C$_{80}$-I. Right: positive-ion MALDI mass spectra of isolated M$_2$TiC@C$_{80}$-I; insets show isotopic distributions and mass numbers of the most intense peaks (marked with the dot).

Figure 2. a) ^{13}C NMR spectrum of ^{13}C-enriched Lu$_2$TiC@C$_{80}$-I, asterisks mark the lines of the solvent and the lock. b) Vis/NIR absorption spectra of M$_2$TiC@C$_{80}$-I in toluene. c) FTIR spectra of M$_2$TiC@C$_{80}$-I (gray: M = Lu; black: M = Dy). The inset in (c) compares two spectra in the range of the Ti=C stretching mode.

the most abundant EMF products for Lu, Dy, Er, Y, and Gd. M$_2$TiC@C$_{80}$-I (Roman number denotes the isomer) is the major or the sole component of the fraction eluting at 36 min. Thus, pure M$_2$TiC@C$_{80}$-I (Lu, Dy, Gd) was obtained from the EMF extract in a single HPLC separation step. For other metals, the main fraction also included a small amount of M$_2$C$_{82}$, which could be then easily removed at the second HPLC step (see the Supporting Information (SI), Figures S2 and S4).

The ionic radius of the lanthanide ion (R^{3+}) plays a crucial role in the absolute yield of EMFs. Lu (R^{3+} = 0.86 Å), Er (0.90 Å), and Dy (0.91 Å) afford similar amounts of M$_2$TiC@C$_{80}$-I per synthesis, the yields of Gd$_2$TiC@C$_{80}$-I (0.94 Å) and Nd$_2$TiC@C$_{80}$-I (0.98 Å) are roughly 6 and 20 times lower than that of Dy$_2$TiC@C$_{80}$-I, respectively, whereas Ce$_2$TiC@C$_{80}$ (1.01 Å) is not produced at all. Yttrium (R^{3+} = 0.90 Å) stands apart as the yield of Y$_2$TiC@C$_{80}$-I is about 4 times lower than that of Dy$_2$TiC@C$_{80}$-I, despite the similar ionic radii of Dy^{3+} and Y^{3+}.

Significant amounts of M$_2$C$_{82}$ and M$_2$C$_{84}$ (presumably dimetallofullerenes M$_2$@C$_{82}$ and carbides M$_2$C$_2$@C$_{82}$) are formed for Lu and Er. Besides, the presence of traces of nitrogen in the generator leads to the formation of nitride clusterfullerene M$_3$N@C$_{80}$. However, the yield of these EMFs decreases with the ionic radius faster than the yield of M$_2$TiC@C$_{80}$-I, and Dy$_2$TiC@C$_{80}$-I can be produced with a high degree of selectivity and relatively high absolute yield. Equally high selectivity is also achieved for Y and Gd (Figure 1), but their overall yield is lower.

The molecular structure of Lu$_2$TiC@C$_{80}$ determined by single-crystal X-ray diffraction and ^{13}C NMR spectroscopy was reported earlier.[16] The Lu$_2$TiC cluster rotates inside the C$_{80}$-I_h(7) fullerene resulting in a simple two-line ^{13}C NMR
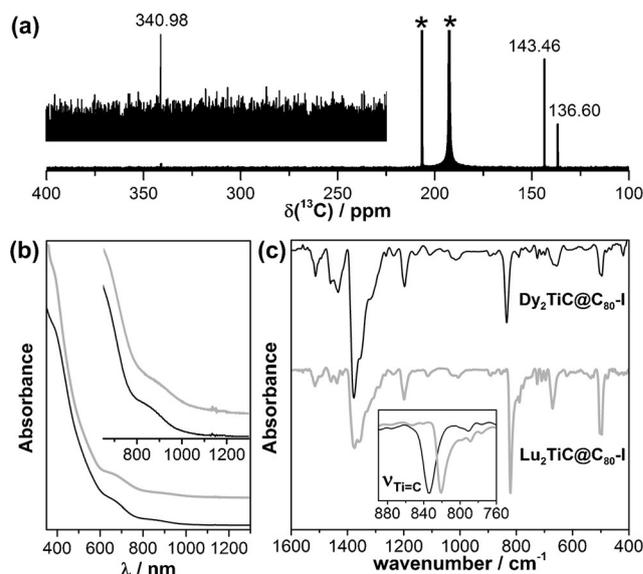
spectrum of the cage carbons. The use of ^{13}C powder for the synthesis of Lu$_2$TiC@C$_{80}$-I in this work allowed detection of the ^{13}C resonance of the central carbon atom at 340.98 ppm (Figure 2). This value is much more positive than the chemical shift of endohedral carbon atoms reported before: 220–260 ppm in M$_2$C$_2$@C$_{2n}$ clusterfullerenes,[8c] 292.4 ppm in YCN@C$_{82}$,[17] and 328.3 ppm in the Sc$_3$C$_2$@C$_{80}^-$ anion.[18] Note that large downfield shifts for metal-bonded carbon atoms are not unusual in Ti alkylidenes with a Ti=C bond.[19] Particularly large shifts in the range of 400–600 ppm are reported for α-C atoms in μ$_3$-bridging alkylidynes of titanium in titanocubane frameworks.[20]

The high selectivity makes Dy$_2$TiC@C$_{80}$-I a suitable synthetic target for further studies of its properties. Comparison of the Vis/NIR and IR absorption spectra prove that the Dy and Lu compounds are isostructural (Figure 2). Both have very similar Vis/NIR spectra with the lowest energy band at 910 nm (Figure 2b) and almost identical vibrational pattern of the fullerene cage (Figure 2c). However, the larger ionic radius of Dy^{3+} pushes the central carbon atom closer to Ti, which results in a higher Ti=C stretching frequency in Dy$_2$TiC@C$_{80}$-I (834 cm^{-1} versus 821 cm^{-1} in Lu$_2$TiC@C$_{80}$-I). Analogous variations of the vibrational frequency with an increase of the lanthanide ionic radius was observed for the Sc−N stretching mode in M$_2$ScN@C$_{80}$.[21] In a similar fashion, isostructurality of other M$_2$TiC@C$_{80}$-I EMFs can be established via their absorption spectra (Figure S7). Besides, all compounds show similar redox behavior with the reversible Ti-based reduction near −1.0 V (vs. Fe(Cp)$_2^{+/0}$ couple) and cage-based oxidation at +0.6 V (Figure 3, Figure S8, and Table 1). Note that reduction potential depends on the size of the lanthanide, whereas the oxidation process is metal-independent.
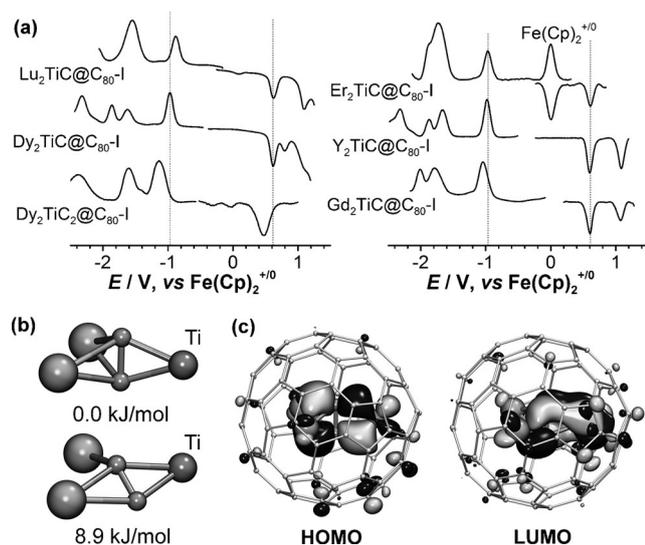
Figure 3. a) Square-wave voltammetry of $M_2TiC@C_{80}$-I (M = Lu, Dy, Er, Y, Gd) and $Dy_2TiC_2@C_{80}$-I measured in *o*-dichlorobenzene/tetrabutyl-ammonium hexafluorophosphate (*o*-DCB/TBAPF$_6$). b) Two conformations of the Lu_2TiC_2 cluster in the DFT-optimized molecular structure of $Lu_2TiC_2@C_{80}$-I (atoms are shown as spheres with the radius decreasing from Lu to Ti to C). c) HOMO and LUMO of $Lu_2TiC_2@C_{80}$-I computed at the PBE/TZVP level.

Table 1: Redox potentials (V) of $M_2TiC@C_{80}$-I, $Dy_2TiC@C_{80}$-II, and $Dy_2TiC_2@C_{80}$-I.[a]

EMF	Ox-II	Ox-I	Red-I	Red-II	Red-III	Red-IV
$Lu_2TiC@C_{80}$-I	1.10	0.63	−0.87	−1.53	–	–
$Er_2TiC@C_{80}$-I		0.62	−0.96	−1.72	–	–
$Y_2TiC@C_{80}$-I	1.07	0.60	−0.99	−1.67	−1.89	−2.32
$Gd_2TiC@C_{80}$-I	1.07	0.60	−1.04	−1.72	−1.91	−2.44
$Dy_2TiC@C_{80}$-I		0.61	−0.97	−1.62	−1.87	−2.33
$Dy_2TiC_2@C_{80}$-I		0.47	−1.14	−1.58	−2.29	–

[a] All potentials are determined by square-wave voltammetry and are reference to the $Fe(Cp)_2^{+/0}$ redox couple; the values for $Lu_2TiC@C_{80}$-I are from Ref. [16].

Owing to the higher selectivity in the synthesis with CH_4 as the reactive gas, other Ln–Ti carbide clusterfullerenes could be detected; this was not possible in the first report on $Lu_2TiC@C_{80}$-I.[16] Mass spectrometry studies proved the formation of $M_2TiC@C_{2n}$ with larger cages (C_{82}, C_{84}), albeit in rather small amounts making their isolation impractical at this moment (see SI). More importantly, we identified the second isomer of $M_2TiC@C_{80}$ and a new type of M-Ti-carbide cluster with one more carbon atom in the structure, $M_2TiC_2@C_{80}$ (the new clusterfullerene also has two isomers, see Figures S1b and S2a). $M_2TiC@C_{80}$-II and $M_2TiC_2@C_{80}$-I have very similar retention times and elute in one fraction (Figures 1 and 4). Dy and Lu EMFs were separated by recycling HPLC as shown in Figures S1 and S3. Figure 4 compares HPLC traces and mass spectra of isolated $Dy_2TiC@C_{80}$-II and $Dy_2TiC_2@C_{80}$-I (each sample still contains a few percent of the other compound). Absorption spectra of $M_2TiC@C_{80}$-II and $M_2TiC_2@C_{80}$-I (M = Dy, Lu) shown in Figure 4b,c lack well-defined features and extend to ca. 1000 nm for the former and ca. 1100 for the
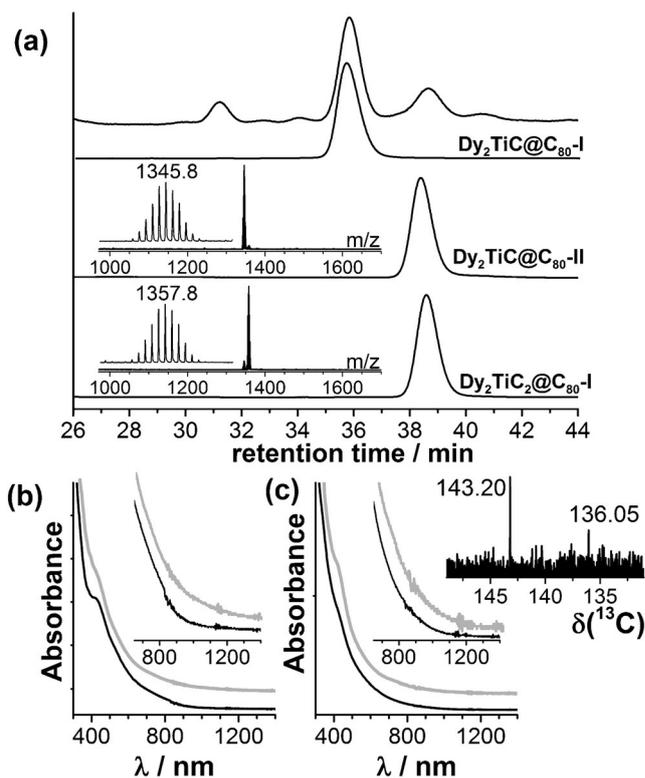

Figure 4. a) HPLC trace of the raw Dy-Ti extract (top) and HPLC curves for individual $Dy_2TiC@C_{80}$-I, $Dy_2TiC@C_{80}$-II, and $Dy_2TiC_2@C_{80}$-I; the insets show their mass spectra. b,c) UV/Vis/NIR absorption spectra of (b) $M_2TiC@C_{80}$-II and (c) $M_2TiC_2@C_{80}$-I (black: M = Dy, gray: M = Lu); the inset shows the ^{13}C NMR spectrum of $Lu_2TiC_2@C_{80}$-I.

latter. The close similarity of the M_2TiC and M_2ScN clusters suggest that $M_2TiC@C_{80}$-II is likely to have a $D_{5h}(6)$ cage. The ^{13}C NMR spectrum of $Lu_2TiC_2@C_{80}$-I (Figure 4c inset) has two ^{13}C signals at 143.20 and 136.05 ppm (versus 143.46 and 136.60 ppm in $Lu_2TiC@C_{80}$-I). Thus, the cage symmetry of $M_2TiC_2@C_{80}$-I can be assigned as $I_h(7)$.

DFT calculations show that the M_2TiC_2 cluster has two conformations with similar energies. In the most stable one, the C_2 unit is perpendicular to the M_2Ti plane and has μ_2-coordination with all metal atoms (Figure 3). In the second one (9 kJ mol^{-1} higher in energy), the C_2 fragment is tilted out of the M_2Ti plane, has μ_2-coordination with Ti and one lanthanide, and μ_1-coordination with another lanthanide. C_2 is likely to exhibit fluxional motion at room temperature. The structure and dynamics of the M_2TiC_2 cluster are similar to those of M_3C_2 clusters in $Sc_3C_2@C_{80}$[22] and $Lu_3C_2@C_{88}$.[23]

$M_2TiC@C_{80}$-I has a cluster-localized LUMO with large contribution of Ti and a fullerene-based HOMO,[16] and similar spatial distribution of the frontier MOs is predicted for $M_2TiC@C_{80}$-II. In $Lu_2TiC_2@C_{80}$-I, both HOMO and LUMO are predominantly localized on the endohedral cluster and have a large contribution of the acetylide fragment. The LUMO of $Lu_2TiC_2@C_{80}$ is to a large extent localized on Ti, whereas in the HOMO both Lu and Ti have comparable contributions (Figure 3). Thus, both reduction and oxidation of $M_2TiC_2@C_{80}$-I are cluster-based processes. $Dy_2TiC_2@C_{80}$-I exhibits two reversible reductions and one oxidation; in
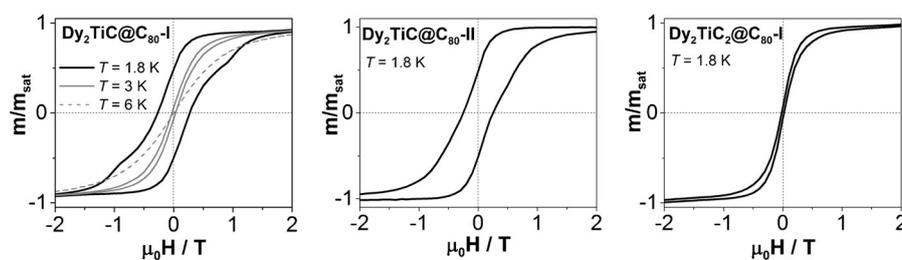
Figure 5. Magnetization curves of $Dy_2TiC@C_{80}$-I, $Dy_2TiC@C_{80}$-II, and $Dy_2TiC_2@C_{80}$-I measured by SQUID. All shown curves are measured at 1.8 K with a sweep rate of $5\ mTs^{-1}$; for $Dy_2TiC@C_{80}$-I the measurements at 3 K and 6 K are also shown.

comparison to $Dy_2TiC@C_{80}$-I, the redox potentials are shifted cathodically by ca. 0.15 V (Figure 3, Table 1).

Recently we have discovered that mixed-metal nitride clusterfullerenes $Dy_xSc_{-x}N@C_{80}$ ($x = 1$–3) exhibit slow relaxation of the magnetization with a temperature-dependent decay rate, that is, they behave as single-molecule magnets (SMMs).[12,24] Of the three nitride clusterfullerenes, $Dy_2ScN@C_{80}$ is the strongest SMM due to the ferromagnetic exchange and dipolar interaction of the two Dy^{3+} ions. Unfortunately, selective synthesis of mixed-metal nitride clusterfullerenes is not possible. The arc-discharge synthesis in the Dy–Sc system always produces a mixture of $Dy_xSc_{3-x}N@C_{2n}$ ($x = 0$–3) compounds with different isomeric structures as well as other cage sizes,[25] and isolation of $Dy_2ScN@C_{80}$ is quite a tedious process. Therefore, the selective synthesis of $Dy_2TiC@C_{80}$-I, which is isostructural to $Dy_2ScN@C_{80}$-I, opens a more convenient route to EMF-based Dy-SMMs as along as the magnetic properties of the two EMFs are similar.

Figure 5 displays the magnetization curve of $Dy_2TiC@C_{80}$-I recorded for different temperatures at a field sweep rate of $5\ mTs^{-1}$. The system shows magnetic hysteresis with a temperature-dependent opening. The observation indicates that the system exhibits a slow relaxation of the magnetization with a decay rate that depends on the temperature. At a constant temperature, the opening is also determined by the field sweep rate as demonstrated in Figure S9. Similar behavior was observed for $Dy_2ScN@C_{80}$ and is characteristic for SMMs. The stability of the remnant magnetization can be quantified by determining the temperature at which the zero-field magnetization relaxation time is 100 s, the so-called 100 s blocking temperature (T_{B100}).[26] In the present case, we obtain $T_{B100} = 1.7$ K for $Dy_2TiC@C_{80}$-I as compared to $T_{B100} = 3.6$ K for $Dy_2ScN@NC_{80}$.[12,26c] The higher T_{B100} value for the nitride clusterfullerene indicates that the nitride ion in the endohedral cluster is advantageous for stronger SMMs.

Isolation of $Dy_2TiC@C_{80}$-II and $Dy_2TiC_2@C_{80}$-I allows us to study how the cage isomerism and the carbide cluster composition affect magnetic properties. Corresponding magnetization curves measured at 1.8 K are shown in Figure 5. The two isomers of $Dy_2TiC@C_{80}$ have a similar field dependence and the same T_{B100} value to within 0.1 K. In contrast, $Dy_2TiC_2@C_{80}$ exhibits a narrower hysteresis than the $Dy_2TiC@C_{80}$ isomers. The T_{B100} value of $Dy_2TiC_2@C_{80}$ is below 1.5 K demonstrating that it is the softest magnet in the series. Thus, substitution of a single carbide ion by an

acetylide unit in the endohedral cluster has an obvious deleterious effect on the SMM properties.

This work shows that lanthanide–Ti carbide clusterfullerenes can be synthesized with high selectivity using methane as a reactive gas. In particular, $Dy_2TiC@C_{80}$-I is the first mixed-metal EMF obtained as a main fullerene product and separated without elaborate chromatographic procedures. Similar to its $Dy_2ScN@C_{80}$ analogue, $Dy_2TiC@C_{80}$-I is a single-molecule magnet. Thus, the class of EMF-SMMs is expanded to carbide clusterfullerenes. The study of the second isomer of $Dy_2TiC@C_{80}$ showed that the carbon cage isomerism has little effect on the magnetic behavior as the two isomers behave similarly. At the same time, we found a strong dependence of SMM properties on the central nonmetal unit: the strength of Dy_2-SMMs is decreases in the series $Dy_2ScN > Dy_2TiC > Dy_2TiC_2$.

[1] S. Stevenson, G. Rice, T. Glass, K. Harich, F. Cromer, M. R. Jordan, J. Craft, E. Hadju, R. Bible, M. M. Olmstead, K. Maitra, A. J. Fisher, A. L. Balch, H. C. Dorn, *Nature* **1999**, *401*, 55–57.

[2] L. Dunsch, M. Krause, J. Noack, P. Georgi, *J. Phys. Chem. Solids* **2004**, *65*, 309–315.

[3] L. Dunsch, S. Yang, L. Zhang, A. Svitova, S. Oswald, A. A. Popov, *J. Am. Chem. Soc.* **2010**, *132*, 5413–5421.

[4] a) B. Q. Mercado, M. M. Olmstead, C. M. Beavers, M. L. Easterling, S. Stevenson, M. A. Mackey, C. E. Coumbe, J. D. Phillips, J. P. Phillips, J. M. Poblet, A. L. Balch, *Chem. Commun.* **2010**, *46*, 279–281; b) S. Stevenson, M. A. Mackey, M. A. Stuart, J. P. Phillips, M. L. Easterling, C. J. Chancellor, M. M. Olmstead, A. L. Balch, *J. Am. Chem. Soc.* **2008**, *130*, 11844–11845.

[5] C. R. Wang, T. Kai, T. Tomiyama, T. Yoshida, Y. Kobayashi, E. Nishibori, M. Takata, M. Sakata, H. Shinohara, *Angew. Chem. Int. Ed.* **2001**, *40*, 397–399; *Angew. Chem.* **2001**, *113*, 411–413.

[6] M. Krause, F. Ziegs, A. A. Popov, L. Dunsch, *ChemPhysChem* **2007**, *8*, 537–540.

[7] T.-S. Wang, L. Feng, J.-Y. Wu, W. Xu, J.-F. Xiang, K. Tan, Y.-H. Ma, J.-P. Zheng, L. Jiang, X. Lu, C.-Y. Shu, C.-R. Wang, *J. Am. Chem. Soc.* **2010**, *132*, 16362–16364.

[8] a) S. Yang, F. Liu, C. Chen, M. Jiao, T. Wei, *Chem. Commun.* **2011**, *47*, 11822–11839; b) A. A. Popov, S. Yang, L. Dunsch, *Chem. Rev.* **2013**, *113*, 5989–6113; c) X. Lu, L. Feng, T. Akasaka, S. Nagase, *Chem. Soc. Rev.* **2012**, *41*, 7723–7760.

[9] Y. Zhang, A. A. Popov, *Organometallics* **2014**, *33*, 4537–4549.

[10] a) Y. Zhang, K. B. Ghiassi, Q. Deng, N. A. Samoylova, M. M. Olmstead, A. L. Balch, A. A. Popov, *Angew. Chem. Int. Ed.* **2015**, *54*, 495–499; *Angew. Chem.* **2015**, *127*, 505–509; b) S. Yang, A. A. Popov, L. Dunsch, *J. Phys. Chem. B* **2007**, *111*, 13659–13663.

[11] N. Chen, E. Y. Zhang, K. Tan, C. R. Wang, X. Lu, *Org. Lett.* **2007**, *9*, 2011–2013.

[12] R. Westerström, J. Dreiser, C. Piamonteze, M. Muntwiler, S. Weyeneth, K. Krämer, S.-X. Liu, S. Decurtins, A. Popov, S. Yang, L. Dunsch, T. Greber, *Phys. Rev. B* **2014**, *89*, 060406.

[13] a) L. Dunsch, S. Yang, *Small* **2007**, *3*, 1298–1320; b) J. Zhang, S. Stevenson, H. C. Dorn, *Acc. Chem. Res.* **2013**, *46*, 1548–1557.

[14] a) C. Chen, F. Liu, S. Li, N. Wang, A. A. Popov, M. Jiao, T. Wei, Q. Li, L. Dunsch, S. Yang, *Inorg. Chem.* **2012**, *51*, 3039–3045; b) S. Yang, C. Chen, A. Popov, W. Zhang, F. Liu, L. Dunsch, *Chem. Commun.* **2009**, 6391–6393.

[15] a) A. A. Popov, C. Chen, S. Yang, F. Lipps, L. Dunsch, *ACS Nano* **2010**, *4*, 4857–4871; b) S. Yang, C. Chen, X. Li, T. Wei, F. Liu, S. Wang, *Chem. Commun.* **2013**, *49*, 10844–10846.

[16] A. L. Svitova, K. Ghiassi, C. Schlesier, K. Junghans, Y. Zhang, M. Olmstead, A. Balch, L. Dunsch, A. A. Popov, *Nat. Commun.* **2014**, *5*, 3568, DOI: 3510.1038/ncomms4568.

[17] S. Yang, C. Chen, F. Liu, Y. Xie, F. Li, M. Jiao, M. Suzuki, T. Wei, S. Wang, Z. Chen, X. Lu, T. Akasaka, *Sci. Rep.* **2013**, *3*, 1487.

[18] Y. Yamazaki, K. Nakajima, T. Wakahara, T. Tsuchiya, M. O. Ishitsuka, Y. Maeda, T. Akasaka, M. Waelchli, N. Mizorogi, H. Nagase, *Angew. Chem. Int. Ed.* **2008**, *47*, 7905–7908; *Angew. Chem.* **2008**, *120*, 8023–8026.

[19] D. J. Mindiola, B. C. Bailey, F. Basuli, *Eur. J. Inorg. Chem.* **2006**, 3135–3146.

[20] a) A. Martín, M. Mena, M. d. C. Morales-Varela, C. Santamaría, *Eur. J. Inorg. Chem.* **2004**, 1914–1921; b) A. Abarca, M. Galakhov, P. Gómez-Sal, A. Martín, M. Mena, J.-M. Poblet, C. Santamaría, J. P. Sarasa, *Angew. Chem. Int. Ed.* **2000**, *39*, 534–537; *Angew. Chem.* **2000**, *112*, 544–547; c) R. Andrés, P. Gómez-Sal, E. de Jesús, A. Martín, M. Mena, C. Yélamos, *Angew. Chem. Int. Ed. Engl.* **1997**, *36*, 115–117; *Angew. Chem.* **1997**, *109*, 72–74.

[21] a) S. Yang, A. A. Popov, C. Chen, L. Dunsch, *J. Phys. Chem. C* **2009**, *113*, 7616–7623; b) S. F. Yang, M. Kalbac, A. Popov, L. Dunsch, *ChemPhysChem* **2006**, *7*, 1990–1995.

[22] a) K. Tan, X. Lu, *J. Phys. Chem. A* **2006**, *110*, 1171–1176; b) Y. Iiduka, T. Wakahara, T. Nakahodo, T. Tsuchiya, A. Sakuraba, Y. Maeda, T. Akasaka, K. Yoza, E. Horn, T. Kato, M. T. H. Liu, N. Mizorogi, K. Kobayashi, S. Nagase, *J. Am. Chem. Soc.* **2005**, *127*, 12500–12501.

[23] W. Xu, T.-S. Wang, J.-Y. Wu, Y.-H. Ma, J.-P. Zheng, H. Li, B. Wang, L. Jiang, C.-Y. Shu, C.-R. Wang, *J. Phys. Chem. C* **2011**, *115*, 402–405.

[24] a) R. Westerström, A.-C. Uldry, R. Stania, J. Dreiser, C. Piamonteze, M. Muntwiler, F. Matsui, S. Rusponi, H. Brune, S. Yang, A. Popov, B. Büchner, B. Delley, T. Greber, *Phys. Rev. Lett.* **2015**, *114*, 087201; b) R. Westerström, J. Dreiser, C. Piamonteze, M. Muntwiler, S. Weyeneth, H. Brune, S. Rusponi, F. Nolting, A. Popov, S. Yang, L. Dunsch, T. Greber, *J. Am. Chem. Soc.* **2012**, *134*, 9840–9843.

[25] T. Wei, F. Liu, S. Wang, X. Zhu, A. A. Popov, S. Yang, *Chem. Eur. J.* **2015**, *21*, 5750–5759.

[26] a) D. Gatteschi, R. Sessoli, J. Villain, *Molecular Nanomagnets*, Oxford University Press, New York, **2006**; b) D. N. Woodruff, R. E. P. Winpenny, R. A. Layfield, *Chem. Rev.* **2013**, *113*, 5110–5148; c) R. Westerström, A. Popov, T. Greber, **2015**, DOI: arXiv:1506.03657.